A Neoarchean Paleomagnetic Pole from the Kisii Series of Western Kenya: Implications for Crustal Mobility

Joseph G. Meert[1], Rob Van der Voo[2] and Jayanti Patel[3]

[1]Department of Geological Sciences, 355 Williamson Hall, University of Florida, Gainesville, FL 32611

[2]Department of Earth and Environmental Sciences, 2534 C.C. Little Bldg. University of Michigan, Ann Arbor, MI 48109

[3]Department of Physics, University of Nairobi, Nairobi, Kenya

Abstract

The Kisii Series lavas of western Kenya were the target of a paleomagnetic study. The Kisii Series is a volcano-sedimentary sequence dated to 2531 ± 3 Ma (U-Pb) that rests unconformably over the Mesoarchean-Neoarchean Nyanzian and Kavirondian Series. The paleomagnetic study reported in this paper expands on an earlier study by Brock et al. (1972) using modern demagnetization and analysis techniques. In spite of the advanced methods, the results of both our new study and the previous study are statistically indistinguishable. We therefore combine the results of both investigations to arrive at a grand mean pole at 7°S, 167° E (A95=7.4°). Field tests are inconclusive in establishing the primary nature of the Kisii pole. We argue for a primary remanence on the basis of a comparison to other paleomagnetic data in Kenya and Tanzania. We examine the relationships between age-equivalent paleomagnetic poles from the Tanzanian, Zimbabwe and Kaapvaal nuclei. Based on this limited dataset, we cannot conclude whether or not the observed apparent polar wander was due to true polar wander or modern-style plate tectonics, such as would be implied by the (variable) apparent polar wander path segments. We favor the latter explanation based on the disparate lengths of the Zimbabwe versus Tanzanian apparent polar wander paths during the 2700-2500 Ma interval.

Keywords: Neoarchean, paleomagnetism, plate tectonics, Protopangea

Introduction

Debates regarding the onset of modern-style tectonics during the Precambrian have blossomed in the past two decades (Piper, 2013; Condie and Kroner, 2008; Condie and Pease, 2009, Davies, 1992; Stern, 2008; Evans and Pisarevsky, 2008; Cawood et al., 2006).

At the extreme ends of the argument are those who advocate modern-style plate tectonics from Archean to present (Bercovici and Ricard, 2014;; Shirey and Richardson, 2011; Cawood et al., 2006) and those who argue that modern style plate tectonics did not begin until ~1000-1100 Ma or perhaps slightly later in the Neoproterozoic (Moores, 1993; Stern, 2005, 2008; Hamilton, 2011; Piper, 2013). Still others advocate a transition from lid-style tectonism to a subduction driven system (Piper, 2013; Moore and Webb, 2013). Many of the arguments are based on thermal models and the evolution of mantle-crust rheology (Bercovici and Ricard, 2014; Korenaga, 2013; Moore and Webb, 2013; Shirey and Richardson, 2011).

Paleomagnetic studies allow for a quantitative assessment of horizontal motion and the relationships between different crustal elements (Evans and Pisarevsky, 2008; Piper, 2010, 2013), but treatment of the data are highly variable in these studies. As an example, Piper (2010) uses a minimal quality filter (i.e. stepwise demagnetization, A95<16°, magnetization interpreted to be primary and ages within ± 200 Ma). It appears that the last criterion (loose age constraints) provides the foundation for Piper's argument favoring long-lived crustal integrity of Protopangea (see discussion in Meert, 2014; Meert and Torsvik, 2003, 2004). In contrast, Evans and Pisarevsky (2008) apply very rigid criteria using only 'key' poles (Buchan et al., 2000). Unfortunately, applying either a highly restrictive or a generously permissive filter to the data results in ambiguous conclusions. Evans and Pisarevsky (2008) conclude that there is a single instance of 'plate-like' motion during the Archean that can be separated from true polar wander. In contrast, Piper (2010) concludes that the Archean and Paleoproterozoic intervals were dominated by 'stagnant-lid' tectonics where the main crustal blocks remained in a semi-rigid configuration. In the Piper (2010) model, the bulk of motion resulted from inertial instabilities leading to true polar wander or, alternatively, motion of the single "Protopangean" lid over the mantle. Piper (2010) argues that modern-style plate tectonics did not begin until the Neoproterozoic.

Paleomagnetic studies on Archean-age rocks may provide quantitative evidence for mobility of the crust; although the studies are often fraught with difficulties. Many of the sequences were deformed and metamorphosed such that the magnetism has been reset to a younger time. In other cases, the paleomagnetic directions are well constrained, but the age of the unit is not known. The Kisii Series in Kenya (figure 1) is a relatively undeformed and

unmetamorphosed volcano-sedimentary sequence. In this paper, we update the results of Brock et al. (1972) who used blanket demagnetization techniques on the Kisii lavas of western Kenya and discuss the implications of our results for the Protopangea model and Archean crustal mobility.

Geology/Tectonics of the Kisii Region

Kabete et al. (2012) summarized recent geochronological work on the Tanzanian craton and the ages quoted in this section and figure 2 are from that compilation. The basement rocks of the Tanzanian craton are composed of the Dodoman gneisses and schists (>3600 to ~3100 Ma). The schists and gneisses are intruded by the so-called 'Older Granites' (3100-2850 Ma) and are unconformably overlain by the Nyanzian System composed of bi-modal volcanic rocks and banded iron formations (2850-2700 Ma). The Nyanzian System is folded, faulted and intruded by granitic rocks. The intrusion of the granitic rocks (2680-2650 Ma) coincides with the major phase of deformation in the Nyanzian rocks (folding and faulting; Kabete et al., 2012; Meert et al. 1994). $^{40}Ar/^{39}Ar$ ages from the Nyanzian basalts in the Kisii region yielded plateau ages between 2670-2680 Ma that were interpreted to reflect the age of metamorphism/deformation (Meert et al., 1994). The Nyanzian System is overlain by the Kavirondian Group (conglomerate and associated sedimentary rocks). The Kavirondian Group is locally intruded by granites and is also folded (Negcu and Gaciri, 1995).

Pinna et al. (2000) provide a useful geological summary of the Kisii Series. Initial mapping of the Kisii Series was conducted by the Geological Survey of Kenya (Shackleton, 1948; Schoeman, 1949; Huddleston, 1951; Saggerson, 1952). The sequence lies unconformably over older granite, gneisses and rocks of the Kavirondian Group and Nyanzian System (figures 1 and 2). From top-to bottom, the Kisii Series is comprised of (a) upper volcaniclastic beds and andesites; (b) Ignimbrites, felsites and rhyolites; (c) arenites; (d) basalts and porphyritic basalts; (e) lower detrital beds. The Kisii Series are intruded by a series of younger dolerite dykes. Localized deformation includes minor tilting and faulting (most units in this study had dips <10°). The age of the minor tilting in the region is not known, but is most probably related to the development of the East African Rift (Tertiary or younger). There are also localized strike-slip and reverse faults along the eastern margin of the basin that formed during the East African Orogeny (Huddleston, 1951; Pinna et al., 2000).

The lack of penetrative deformation and regional metamorphism led many to correlate the Kisii Series with other cratonic cover sequences in the Tanzanian craton (see summary in Pinna et al., 2000). Huddleston (1951), following the leads of Shackleton (1948) and Schoeman (1949) equated the rocks in the Kisii Quadrangle to the Bukoban Series in Tanzania and Burundi. Geochronological studies on the Bukoban rocks were conducted on the Gagwe and Kabuye lavas in Tanzania and Burundi. These rocks yielded limited, but consistent K-Ar ages between 810-822 Ma (recalculated using modern decay constants; Briden et al., 1971; Cahen and Snelling, 1974, Cahen et al., 1984). Attempts to date the Kisii lavas using K-Ar methods yielded a much wider range of ages between 546-1283 Ma (Cahen and Snelling, 1966; Briden et al., 1971; Charlton, 1973; Meert, 1993). The traditional correlation between the Bukoban and Kisii Series was first questioned by Brock et al. (1972) and Brock and Piper (1972). In companion papers, Brock et al. (1972) and Brock and Piper (1972) cited 'reliable' K-Ar ages from the Kisii lavas of ~930 Ma published the previous year by Briden et al. (1971) as proof that the Bukoban and Kisii rocks were of significantly different ages. They further showed that paleomagnetic directions from the Bukoban Sequence (including the Gagwe lavas) were distinct from the Kisii lavas pole. The paleomagnetic argument was the most compelling as Charlton (1973) and Meert (1993) showed that the K-Ar system in the Kisii lavas was highly disturbed. Neither study was able to isolate well-defined $^{40}Ar/^{39}Ar$ plateaus in whole rock nor in mineral separates. Total $^{40}Ar/^{39}Ar$ fusion ages in those two studies (i.e. K-Ar equivalent ages) ranged from 823-1283 Ma. Meert (1993) also attempted to date the Kisii Series using the $^{147}Sm/^{143}Nd$ isotopic system on whole-rock/clinopyroxene pairs and obtained widely disparate model ages between 2208-3215 Ma.

More recently, zircon data from the upper part of the Kisii lava sequence (Ikonge Ignimbrite) yielded a U-Pb single zircon evaporation age of 2531 ± 3 Ma (Pinna et al., 2000). Pinna et al. (2000) concluded that the Kisii Series volcano-sedimentary sequence was produced during Late Archean subduction coinciding with the waning phases of the Victorian Orogeny.

There are also now more precise age constraints on the Bukoban volcanic rocks (i.e. Gagwe lavas). Deblond et al. (2001) argued that a 795 ± 7 Ma ($^{40}Ar/^{39}Ar$) age on Gagwe intrusive equivalents in Burundi was the best estimate for the age of the lavas and that the previously published K-Ar ages suffered from excess argon. Wingate and Pisarevsky (2010) dated the Luakela volcanics (Congo) at 765 ± 7 Ma and demonstrated that the paleomagnetic directions in those volcanics are identical to the Bukoban directions (e.g. Gagwe lavas; Piper, 1972; Meert et al., 1995).

Given the new geochronological data discussed above and the known disparity between the paleomagnetic directions observed in the Kisii Series (Brock et al., 1972, this study) and the Bukoban sequence (Piper, 1972; Meert et al., 1995), the correlation between the two sequences is no longer tenable (Figure 3).

Additional paleomagnetic studies in the region were conducted on granitic rocks that intrude the Kavirondian and Nyanzian rocks (Patel and Raja, 1979; Patel, 1989) and the Nyanzian volcanic rocks (Meert et al., 1994). The paleomagnetic directions obtained from the granites that were intruded prior to folding of the Nyanzian and Kavirondian Systems are no longer considered valid (Figure 3; see also Meert et al., 1994).

Methods

A total of 90 samples were collected from 10 sites in the Kisii lava sequence. Eight of the sites sampled the lower basaltic flows and two sites were taken from the more felsic upper part of the Series (Figure 1). Samples were collected in the field using a gasoline-powered drill and oriented using solar and magnetic compass. All samples were then cut to standard-sized cores and the natural remanent magnetization (NRM) was measured on either a ScT cryogenic or Schonstedt spinner magnetometer at the University of Michigan's paleomagnetic laboratory. Thermal and alternating field (AF) demagnetization was carried out on a pilot selection of samples to choose the optimal method of magnetic cleaning. Both methods proved to be equally successful, but the majority of samples were treated thermally because a more complete decay of the NRM could be achieved. Rock magnetic studies included isothermal remanence acquisition and Curie temperature analyses. IRM was stepwise induced up to 1.0 T using an ASC-Scientific pulse magnetizer (ASC Scientific) at the University of Florida. Susceptibility-temperature measurements (Curie runs) were conducted on a KLY-3S bridge with CS-3 furnace (Agico Instruments) at the University of Florida.

Results

Paleomagnetic Results

Of the 90 samples, 71 samples showed easily interpretable results (figures 4a-c, 5a-c, 6a-c and 7a-c). Some samples exhibited near uni-vectorial decay to the origin (figure 4a) while others showed one or two lower-temperature overprints (<520 C; figures 5a, 6a and 7a). The most consistent overprint (<300° C) was directed to the north and shallowly up (recent field overprint; see figures 5a, 6a for example). The remaining 19 samples yielded only a recent field overprint (north-shallow) or chaotic behavior during demagnetization and are not considered further in the results.

The mean directions for the high-temperature/coercivity components are given in Table 1. Two sites in the more acidic lavas showed directions that were reverse (west-down) as compared to the remaining eight sites in the lavas (east-up). After inverting the directions from the acidic lavas, the mean in-situ direction was calculated at Dec=103°, Inc=-53° (k=43, α_{95}=7.4°; Fig 8a). After correcting for minor tilt, the mean direction is Dec=99°, Inc=-59° (k=52, α_{95}=6.7°; Fig 8b). There is a slightly better grouping of directions tilt-corrected coordinates and so we use the tilt-corrected direction in the discussion. The resultant paleomagnetic pole falls at 9° S, 166° E (A95=9°).

Our grand mean direction is nearly identical to the directions obtained by Brock et al. (1972; Table 1). The paper by Brock et al. (1972) does not report individual sample results (or α_{95} values). Based on the sketch map in Brock et al. (1972) and our own field observations, it appears that our sites 5 and 9 are identical to sites 13 and 4 sampled by

Brock et al. (1972). Because of the limited data available in the original study, we calculated a mean for our sites and a mean for the Brock et al. (1972) sites separately and then combined both into a grand mean. The grand mean (GM) calculated from both studies yields a Dec=99°, Inc=-59° (k=37, α_{95}=5.6°) with a resultant paleomagnetic pole at 7° S, 167° E (A95=7.4°).

Rock Magnetic Results

Rock magnetic studies carried out on a selected suite of samples from the andesites, felsites and basalts indicate that there are multiple remanence carriers in the samples. Isothermal remanence acquisition curves on basaltic samples (fig. 9) all show saturation by 0.2-0.3 T. This rapid saturation in relatively low applied fields is consistent with magnetite/low-Ti magnetite as a main carrier of remanence. Magnetite is also indicated in nearly all of the demagnetization intensity decay plots (figs. 5b, 6b and 7b) although an intensity decay at around 300-350° C (figs. 5b,7b) may indicate the presence of pyrrhotite in several samples. Curie temperature runs were conducted on a felsite sample (figs. 10a,b), a porphyritic basalt sample (figs. 10c,d) and a basalt sample (figs. 10e, f). All samples indicate some alteration during heating of the sample (compare susceptibility values in the heating versus cooling curves). The felsite sample shows a Curie temperature (heating) of ~580° C typical of magnetite with an indication of a small amount of hematite (figs. 10a,b). The porphyritic basalt shows no clear Curie temperature during the heating phase, but upon cooling there is an indication of both hematite and magnetite (figs. 10c,d). The basalt sample shows a Curie temperature of ~570° C in the heating curve with some hematite present (fig. 10e). The cooling curve also shows the presence of both hematite and magnetite (fig. 10f).

Discussion

Our study, combined with the earlier results published by Brock et al. (1971) refine the pole for the Kisii lavas. Field tests to constrain the age of the Kisii pole are indeterminate. Correction for local tilt results in a slightly better, but statistically insignificant, clustering (k=32 *in-situ*; k=37 tilt-corrected; Figs. 8a,b). We note that two sites in the upper part of the sequence are of the opposite polarity to the lower basaltic units and therefore the magnetization was acquired during at least one field reversal.

We argue for a near primary magnetization on the following basis: (a) metamorphism in the Kisii Series resulted from syn-genetic hydrothermal activity (forming the famous Kisii soapstone); (b) the Kisii Series was only slightly affected (by normal faulting) during the development of the East African rift; (c) the paleomagnetic directions in the Kisii Series are distinct from expected Miocene-recent directions in the East African rift (fig. 3); (d) the only structures in the Kisii Series associated with the East African Orogeny are to the East of the study area (Aswa shear zone and Nandi Escarpment; Hetzel and Strecker, 1994; Sanders, 1965) (g) paleomagnetic directions from the later stages of the East African Orogeny in Kenya are distinct from the Kisii pole (Meert et al., 1996; fig. 3); (f) clasts in the underlying Kavirondian conglomerate are not remagnetized and; (f) The underlying Nyanzian lavas have a distinct paleomagnetic pole with field tests/geochronology constraining the age of magnetization to ~2670 Ma (fig. 3). According to Van der Voo's (1990) reliability criteria, the Kisii Series is assigned a Q-factor=5. The main argument against a primary magnetization is that the Kisii pole falls on the apparent polar wander path for Gondwana ~530-520 Ma (Meert and Van der Voo, 1996). We treat the Kisii pole as a primary magnetization in the following discussion.

During the most recent Nordic paleomagnetic workshop all Archean-age poles were reviewed and ranked by committee. In the 2500-2600 Ma range, only 5 poles were considered 'key' for this interval. Of the 5 poles, 3 are from Fennoscandia, one from the Superior craton and one from the Zimbabwe craton. It is very difficult with the limited database to discuss crustal mobility or plate reconstructions. Three of the Fennoscandian poles are ~2500 Ma age, but each of the intrusions shows a very different paleomagnetic pole (Mertanen et al., 2006; Arestova et al., 2002; Pechersky et al., 2004). The Ptarmigan mean pole from the Superior craton (2505 Ma; Evans and Halls, 2010) is considered reliable mainly due to its proximity to the slightly younger Matachewan dykes pole at 2466 Ma. At this point, we feel it is premature to evaluate potential relationships between the Tanzanian craton and Fennoscandia/Superior.

It is possible to expand the database slightly and compare paleomagnetic poles from the Kaapvaal, Tanazanian and Zimbabwe nuclei in the 2500-2700 Ma interval. In the following analysis, we use paleomagnetic poles from the African nuclei (Q≥4) which must include a reliable age; Table 2). There are two poles from the Tanzanian craton, two poles from the Zimbabwe craton and three poles from the Kaapvaal craton. The three poles from the Kaapvaal craton are of similar age, but the pole from the Mbanane pluton is different from the other two poles (Allanridge basalts and Rykoppies dykes; Table 2). Because of the lack of structural control on the pluton, we prefer comparisons to the dykes and basalts in our analysis.

If we assume Protopangea integrity during the Late Archean (Piper, 2010), then similar-age poles from the Tanzanian, Zimbabwe and Kaapvaal nuclei should be positioned in the same location. Based on single poles at ~2680 Ma from the three nuclei, such an integrity is not supported (figs. 11 and 12; Table 2). We do note that the differences between the Zimbabwe and Kaapvaal cratons poles are only slightly larger than the maximum error on the pole positions (see Table 3).

For the ~2550 Ma time period, the pole from the Kisii lavas and the Great Dyke mean pole (Table 2 and 3) show a clear difference (angular distance between the two poles is at least 62°) indicating that the two regions were not in their present-day configuration as required by the Protopangea hypothesis. Furthermore, the APWP length for the pair of Zimbabwe poles (Belingwe-Great dyke mean) is 124° versus only 27° for the Tanzanian pair (Nyanzian-Kisii). Thus, based on this limited dataset, it would appear that the Zimbabwe and Tanzanian cratons were most likely (a) moving independently and (b) moving as rigid blocks as opposed to true polar wander. The dataset, while limited, does not support the Protopangea hypothesis (Piper, 2010) where the cratons must remain in a rigid configuration throughout the Archean and Paleoproterozoic. Figure 12 shows the three nuclei reconstructed according to the paleomagnetic data in Table 2. In the reconstruction, we have positioned according to a particular polarity choice and attempted to minimize the longitudinal misfit between the Protopangean configuration (essentially the modern-day positions). Given the usual caveats (i.e. polarity choice, freedom of longitude, errors in pole positions), it is possible to closely approximate the present-day relationships between the Tanzanian craton and the Zimbabwe craton at ~2.5 Ga (Figure 12b), but not at ~2.7 Ga (figure 12a).

Conclusions

We report an updated pole from the Kisii lavas in western Kenya at 7° S, 167° E (A95=7.4°). Limited paleomagnetic data from the Tanzanian, Zimbabwe and Kaapvaal nuclei imply that their present-day geographic distribution was different from that during the Archean; although by choosing a specific polarity and longitudinal placement, it is possible to come close to the present-day geometry at 2.5 Ga. This conclusion negates the specific Protopangea model of Piper (2010) which requires poles to fall along a defined apparent polar wander path. It is more difficult to ascertain the nature of motion implied by these data although true polar wander during the 2700-2500 Ma range is difficult to reconcile with the APW lengths of the Tanzanian and Zimbabwe cratons. As future work provides additional quality poles for the Neoarchean, it may be easier to establish the nature of continental motion implied by these data.

Acknowledgements: Funding for the research in this project was provided by grants from the Geological Society of America (to JGM), Sigma Xi (to JGM), Scott Turner Fund (to JGM and RVDV), University of Michigan Rackham Dissertation Fellowship (to JGM), the Foundation "Stichting Dr. Schürmannfonds", grant no. 1993/02 (to RVDV) and the National Science Foundation grant EAR92-05815 (to RVDV). All conclusions in this paper reflect those of the authors and not the funding agencies.

References

Arestova, N.A., Khramov, A.N., Gooskova, E.G., Iosifidi, A.G., 2002. New paleomagnetic evidence from the Early Proterozoic (2.5-2.46 Ga) Mount Generalskaya and Imandra layered intrusions, Kola Peninsula, Fizika Zemli, 38, 65-76.

Bercovici, D. and Ricard, Y., 2014. Plate tectonics, damage and inheritance, Nature, 508, 513-516.

Briden, J.C., Piper, J.D.A., Henthorn, D.I. and Rex, D.C., 1971. New paleomagnetic results from Africa and related potassium-argon age determinations. 15th Annual Report Research Institute of African Geology, University of Leeds, 46-50.

Brock, A., Raja, P.K.S., Vise, J.B., 1972. The palaeomagnetism of the Kisii Series, western Kenya. Geophysical Journal of the Royal Astronomical Society, 28, 129-137.

Buchan, K.L., Mertanen, S., Park, R.G., Pesonen, L.J., Elming, S.A., Abrahamsen, N., Bylund, G., 2000. Comparing the drift of Laurentia and Baltica in the Proterozoic: The importance of key paleomagnetic poles, Tectonophysics, 319, 167-198.

Cahen, L. and Snelling, N.J. 1974. Potassium-argon ages and additions to the stratigraphy of the Malagarasian (Bukoban System of Tanzania) of SE Burundi, Journal of the Geological Society of London, 130, 461-470.

Cahen, L., Snelling, N.J., Delhal, J., Vail, J.R., 1984. The Geochronology and Evolution of Africa, Clarendon Press, Oxford (UK), 512 pp.

Cawood, P., Kroner, A., Pisarevsky, S.A., 2006. Precambrian plate tectonics:criteria and evidence, GSA Today, 16, 4-11.

Charlton, S., 1973. Limitations of the Argon-39 method on Precambrian dolerites. 16th Annual Report Research Institute of African Geology, University of Leeds, 45-47.

Deblond, A., Punzalan, L.E., Boven, A., Tack, L., 2001. The Malagarazi Supergroup of southeast Burundi and its correlative Bukoba Supergroup of northeast Tanzania: Neo and Mesoproterozoic chronostratigraphic constraints from Ar-Ar ages on mafic intrusive rocks, Journal of African Earth Sciences, 32, 435-449.

De Kock, M., Evans, D.A.D., Beukes, N.J., 2009. Validating the existence of Vaalbara in the Neoarchean, Precambrian Research, 174, 145-154.

Evans, D.A.D., Pisarevsky, S.A., 2008. Plate tectonics on early Earth?, Geological Society of America Special Paper 440, 249-263.

Hamilton WB. 2011. Plate tectonics began in Neoproterozoic time, and plumes from deep mantle have never operated. Lithos 123, 1–20.

Hetzel, R. and Strecker, M.R., 1994. Late Mozambique Belt structures in western Kenya and their influence on the evolution of the Cenozoic Kenya Rift, Journal of Structural Geology, 16, 189-201.

Huddleston, A., 1951. Geology of the Kisii District, Report #18, Geological Survey of Kenya, Government Printer, Nairobi, 65 pp.

Korenaga, Y., 2013. Initiation and evolution of plate tectonics on Earth: Theories and observations, Annual Reviews of Earth and Planetary Sciences, 41, 117-151.

Meert, J.G., 1993. Precambrian Tectonics: Some constraints from paleomagnetic studies in North America and Africa (dissertation), University of Michigan Publications, Ann Arbor, MI, pp. 129-140.

Meert, J.G., Van der Voo, R. and Patel, J.P., 1994. Paleomagnetism of the Late Archean Nyanzian System, western Kenya, Precambrian Research, 69, 113-131.

Meert, J.G., Van der Voo, R., Ayub, S., 1995. Paleomagnetic investigation of the Neoproterozoic Gagwe lavas and Mbozi Complex, Tanzania and the assembly of Gondwana, Precambrian Research, 74, 225-244.

Meert, J.G. and Van der Voo, R., 1996. Paleomagnetic and $^{40}Ar/^{39}Ar$ study of the Sinyai dolerite, Kenya: Implications for Gondwana assembly, Journal of Geology, 104, 131-142.

Meert, J.G. and Torsvik, T.H., 2003. The making and unmaking of a supercontinent:Rodinia Revisited, *Tectonophysics,* 375, 261-288.

Meert, J.G. and Torsvik, T.H., 2004. Reply to JDA Piper: The making and unmaking of a Supercontinent, *Tectonophysics*, 383, 99-103.

Meert, J.G., 2003. A synopsis of events related to the assembly of eastern Gondwana, Tectonophysics, 362, 1-40.

Meert, J.G., 2014. Strange Attractors, Spiritual Interlopers and Lonely Wanderers: The Search for Pre-Pangæan Supercontinents. Geoscience Frontiers, 5, 155-166.

Mertanen, S., Vuollo, J.I., Huhma, H., Arestova,. N.A., Kovalenko, A., 2006. Early Paleoproterozoic-Archean dykes and gneisses in Russian Karelia of the Fennoscandian shield-new paleomagnetic isotopic age and geochemical investigations, Precambrian Research, 144, 239-260.

Moore, W.B., Webb, A.A.G., 2013, Heat-pipe Earth. Nature, 501, p. 501-505.

Moores, E.M., 1993. Neoproterozoic oceanic crustal thinning, emergence of continents and the origin of Phanerozoic ecosystems: A model, Geology, 21, 5-8.

Patel, J.P. and Raja, P.K.S., 1979. A palaeomagnetic study of lower Proterozoic granites from western Kenya, Geophysical Journal of the Royal Astronomical Society, 58, 279-286.

Patel, J.P., 1989. Paleomagnetic results from late Archean and Early Proterozoic granites from southwestern Kenya, Journal of African Earth Sciences, 9, 97-100.

Pechersky, D.M., Zakharov, V.S., Lyubushin, A.A., 2004. Continuous record of geomagnetic field variations during cooling of the Monchegorsk, Kivakka and Bushveld Early Proterozoic layered intrusions, Russian Journal of Earth Science, 6, 391-456.

Pinna, P., Cocherie, A., Thieblemont, D., Jezequel, P., 2000. The Kisii Group of western Kenya: an end Archean (2.53 Ga) late orogenic volcano sedimentary sequence, Journal of African Earth Sciences, 30, 79-97.

Piper, J.D.A., 1972. A paleomagnetic study of the Bukoban System, Tanzania. Geophysical Journal of the Royal Astronomical Society, 28, 111-127.

Piper, J.D.A., 2010. Protopangea:Paleomagnetic definition of Earth's (mid-Archean-Paleoproterozoic) oldest supercontinent, Journal of Geodynamics, 50, 154-165.

Piper, J.D.A., 2013. A planetary perspective on Earth Evolution: Lid tectonics before plate tectonics, Tectonophysics, 589, 44-56.

Sanders, L.D., 1965. Geology of the contact between the Nyanza shield and the Mozambique Belt in western Kenya, Geological Survey of Kenya Bulletin #7, 45 pp.

Saggerson, E.P., 1952. Geology of the Kisumu District, Report #21, Geological Survey of Kenya, Government Printer, Nairobi, 84 pp.

Schoeman, J.J., 1949. Geology of the Sotik District, Report #16, Geological Survey of Kenya, Government Printer, Nairobi, 39 pp.

Shackleton, R.M., 1948. The geology of the Migori gold belt, Report #10, Geological Survey of Kenya, Government Printer, Nairobi, 60 pp.

Shirey, S.B. and Richardson, S.H., 2011. Start of the Wilson Cycle at 3.0 Ga shown by diamonds from subcontinental mantle, Science, 333, 434-436.

Stern, R.J. 2005. Evidence from Ophiolites, Blueschists, and Ultra-High Pressure Metamorphic Terranes that the Modern Episode of Subduction Tectonics Began in Neoproterozoic Time. Geology 33, 557-560.

Stern, R.J. 2008. Modern-Style Plate Tectonics Began in Neoproterozoic Time: An Alternative Interpretation of Earth's Tectonic History. Condie, K., and Pease, V., eds, When did Plate Tectonics Begin?, Geological Society of America Special Paper 440, 265-280.

Strik, G., de Wit, M.J., Langereis, C.G., 2007. Paleomagnetism of the Neoarchean Pongola and Ventersdorp Supergroups and an appraisal of the 3.0-1.9 Ga apparent polar wander path of the Kaapvaal craton, southern Africa, Precambrian Research, 153, 96-115.

Figure Legends

Figure 1. (a) Geological sketch map of the sampling region (after Huddleston, 1951 and Schoeman, 1949). Sampling sites given as white squares, geochronology sampling site given by red star (Pinna et al., 2000). (b) Inset map showing the study area in a more regional context including the Tanzanian, Zimbabwe and Kaapvaal nuclei.

Figure 2. Generalized stratigraphy of the Kisii region. Ages are summarized in Kabete et al. (2012) and/or Meert et al. (1994).

Figure 3: Plot of the Kisii lavas paleomagnetic pole along with previously published poles from Kenya/Tanzania and the Late Ediacaran-Cambrian APWP for Gondwana.

Figure 4: (a) Orthogonal vector diagram for sample VKC-22; (b) Intensity decay plot and; (c) stereoplot for sample VKC-22. Closed/Open circles on stereoplots represent positive/negative inclinations.

Figure 5: (a) Orthogonal vector diagram for sample VKC-45; (b) Intensity decay plot and; (c) stereoplot for sample VKC-45. Symbols same as in figure 3.

Figure 6: (a) Orthogonal vector diagram for sample VKC-39; (b) Intensity decay plot and; (c) stereoplot for sample VKC-39. Symbols same as in figure 3

Figure 7: (a) Orthogonal vector diagram for sample JKA-3; (b) Intensity decay plot and; (c) stereoplot for sample JKA-3. Symbols same as in figure 3.

Figure 8: (a) Stereoplot showing mean site directions and α_{95} errors in-situ; (b) Stereoplot showing mean site directions and α_{95} errors in tilt-corrected coordinates; (c) plot of VGP's calculated from individual sites (red=study by Brock et al., 1972; Navy=this study). See Table 1 for individual results.

Figure 9: Isothermal remanence acquisition curves for a variety of samples used in this study. All show saturation by 0.3 Tesla.

Figure 10: Curie temperature runs for (a) heating curve for felsite; (b) cooling curve for felsite ; (c) heating curve for porphyritic basalt; (d) cooling curve for porphyritic basalt; (e) heating curve for basalt; (f) cooling curve for basalt.

Figure 11: Poles from the Tanzanian, Zimbabwe and Kaapvaal cratons for the 2700-2500 Ma intervals.

Figure 12: (a) Reconstruction of the Kaapvaal, Zimbabwe and Tanzanian cratons at ~2700 Ma based on the paleomagnetic poles listed in Table 2. K27a=Rykoppies pole; K27b=Allanridge basalts; Z27=Belingwe komatiites; T27=Nyanzian lavas. The outline of modern-day Africa is reconstructed to the Nyanzian pole for ease of evaluating the Paleopangean misfit; (b) Reconstruction of the Zimbabwe and Tanzanian cratons at ~2550 Ma based on paleomagnetic poles in Table 2. Z25=Great dyke mean; T25=Kisii lavas. The outline of modern-day Africa is reconstructed to the Kisii pole for ease of evaluating the Paleopangean misfit.

Graphical Abstract (for review)

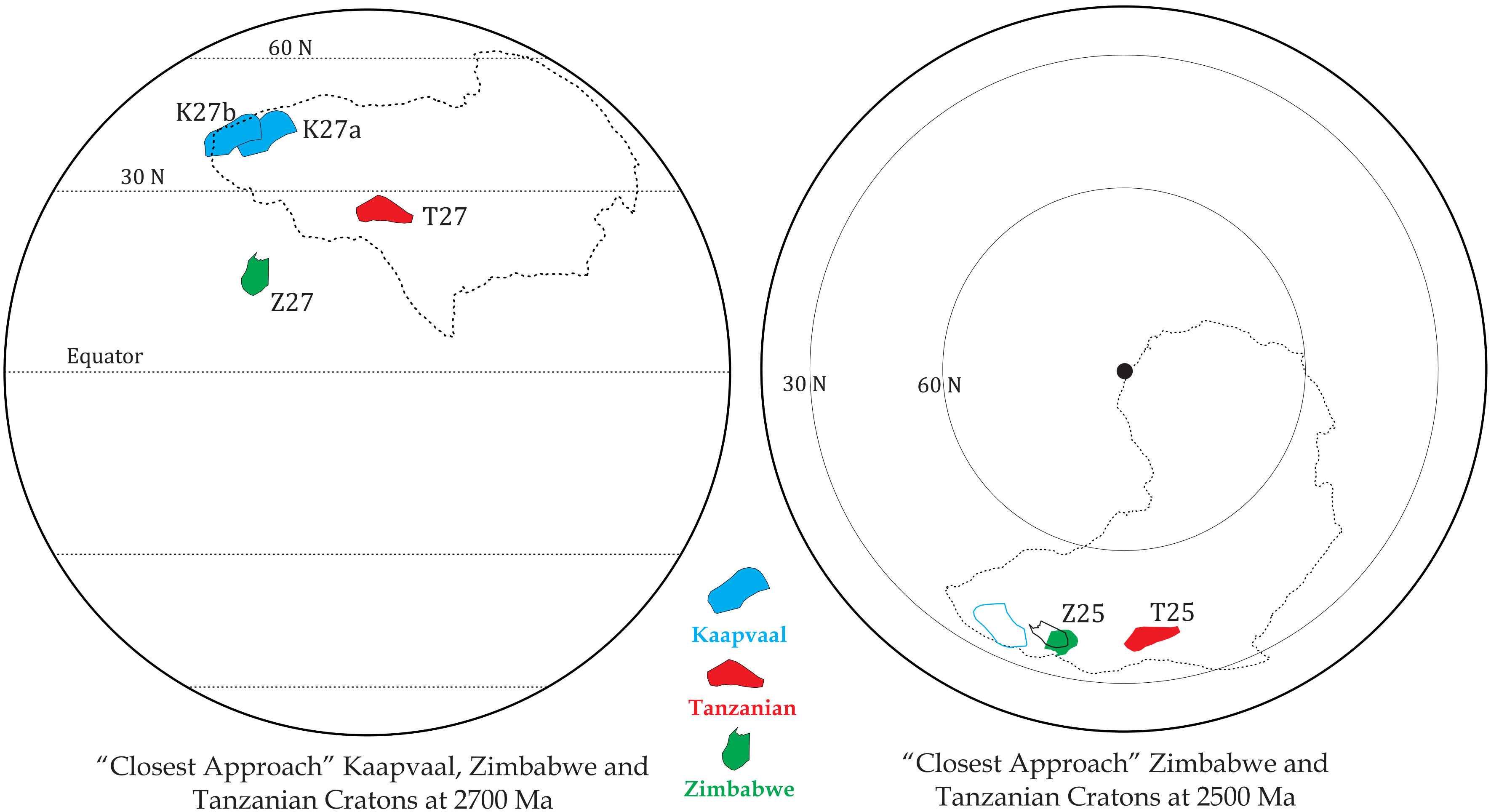

"Closest Approach" Kaapvaal, Zimbabwe and Tanzanian Cratons at 2700 Ma

"Closest Approach" Zimbabwe and Tanzanian Cratons at 2500 Ma

Table1

Table 1.

Site	n/N	Dg	Ig	Ds	Is	K	α_{95}	Plat	Plong	dp	dm
1	8/9	94°	-51°	88°	-58°	23	10°	2° N	163° E	11°	15°
2*	9/9	122°	-37°	112°	-46°	47	5°	19° S	154° E	4°	6°
4	6/6	102°	-53°	92°	-61°	9	19°	1° S	168° E	22°	29°
7	6/9	101°	-53°	103°	-57°	12	16.5°	10° S	163° E	18°	24°
9	7/7	104°	-80°	117°	-85°	228	3.5°	4° S	206° E	7°	7°
10*	6/11	100°	-36°	97°	-44°	14	15.3°	6° S	151° E	12°	19°
11	9/9	96°	-30°	94°	-37°	32	8.3°	4° S	145° E	6°	10°
13	5/9	106°	-54°	101°	-62°	31	11.3°	8° S	169° E	14°	18°
15*	7/11	93°	-71°	76°	-78°	63	6.7°	6° S	192° E	12°	13°
BMean	*9 Sites*	*103°*	*-52°*	*99°*	*-59°*	---	---	*7° S*	*166° E*	*A95=13.2°*	
4	4/6	106°	-48°	102°	-53°	197	6°	9° S	159° E	6°	8°
5	7/9	111°	-54°	120°	-58°	76	9°	23° S	168° E	10°	13°
6	8/8	87°	-62°	97°	-69°	288	3°	4° S	177° E	4°	5°
7	16/16	105°	-42°	103°	-53°	66	5°	11° S	158° E	5°	7°
8	11/15	103°	-36°	105°	-45°	155	5°	13° S	153° E	4°	6°
9	8/10	106°	-53°	97°	-61°	120	6°	5° S	167° E	7°	9°
12	4/7	99°	-60°	106°	-53°	111	9°	13° S	160° E	9°	13°
13	4/7	72°	-75°	67°	-80°	516	4°	9° N	195° E	7°	8°
14	5/6	286°	48°	277°	52°	201	7°	6° S	158° E	7°	10°
15	4/6	291°	51°	282°	54°	87	8°	10° S	160° E	8°	11°
MMean	*10 Sites*	*103°*	*-53°*	*99°*	*-59°*	---	---	*9° S*	*166° E*	*A95=9°*	
Grand Mean	**19 Sites**	**103°**	**-53°**	**98°**	**-59°**	**---**	**---**	**7° S**	**167° E**	**A95=7.4°**	

N=number of samples collected; n=number of samples used in study; Dg=declination in geographic coordinates; Ig=inclination in geographic coordinates; Ds=declination in stratigraphic coordinates; Is=Inclination in stratigraphic coordinates; k=Fisher's (1953) kappa precision parameter; α_{95}=cone of 95% confidence about the mean direction; Plat=Pole latitude; Plong=Pole longitude; dp,dm= cone of 95% confidence about the virtual geomagnetic pole in the co-latitude direction (dp) and orthogonal to the co-latitude direction (dm); A95= 95% confidence circle about the mean paleomagnetic pole. BMean=Mean from the study of Brock et al. (1972); MMean= mean from sites sampled for this study.

*Recalculated from the original study.

Table2

Table 2. Selected Poles From the Tanzanian, Zimbabwe and Kaapvaal Cratons

Pole Name	**Craton**	**Age**	**Plat**	**Plong**	**A95**	**Q-rating**	**Reference**
Nyanzian Lavas	Tanzanian	2680 Ma	-14°	330°	6°	6	Meert et al., 1994
Kisii Lavas	Tanzanian	2531 Ma	7°	347°	7°	5	This study; Brock et al., 1972
Belingwe	Zimbabwe	2692 Ma	-45°	303°	19°	4	Yoshihara and Hamano, 2004
Great Dyke Mean	Zimbabwe	2574 Ma	22°	060°	3°	5	Nordic Working Group 2014
Mbanane Pluton	Kaapvaal	2687 Ma	-20°	286°	5°	4	Layer et al., 1989
Rykoppies dykes	Kaapvaal	2681 Ma	-62°	336°	7°	6	Lubnina et al., 2010
Allanridge basalts	Kaapvaal	2642 Ma	-69°	346°	4°	5	De Kock et al., 2009

Plat=pole latitude; Plong=pole longitude; A95=cone of 95% confidence about the mean pole; Q-rating according to Van der Voo (1990)

Table 3. Great Circle Analysis

Pole A	Pole B	Age	Great Circle Distance between poles
Nyanzian Lavas (T)	Belingwe (Z)	2680 Ma	38° (min 14°)
Nyanzian Lavas (T)	Rykoppies (K)	2680 Ma	48° (min 34°)
Nyanzian Lavas (T)	Allanridge (K)	2680 Ma	56° (min 46°)
Nyanzian Lavas (T)	Mbanane (K)	2680 Ma	42° (min 31°)
Belingwe (Z)	Rykoppies (K)	2680 Ma	25° (min 0°)
Belingwe (Z)	Allanridge (K)	2680 Ma	32° (min 13°)
Belingwe (Z)	Mbanane (K)	2680 Ma	29° (min 5°)
Kisii (T)	Great Dyke (Z)	2550 Ma	73° (min 62°)
Belingwe (Z)	Great Dyke (Z)	Δ=118 Ma	124°
Nyanzian (T)	Kisii Lavas (T)	Δ=149 Ma	27°

Note: The minimum distance is based on α_{95} error envelopes between the two poles.

Figure1

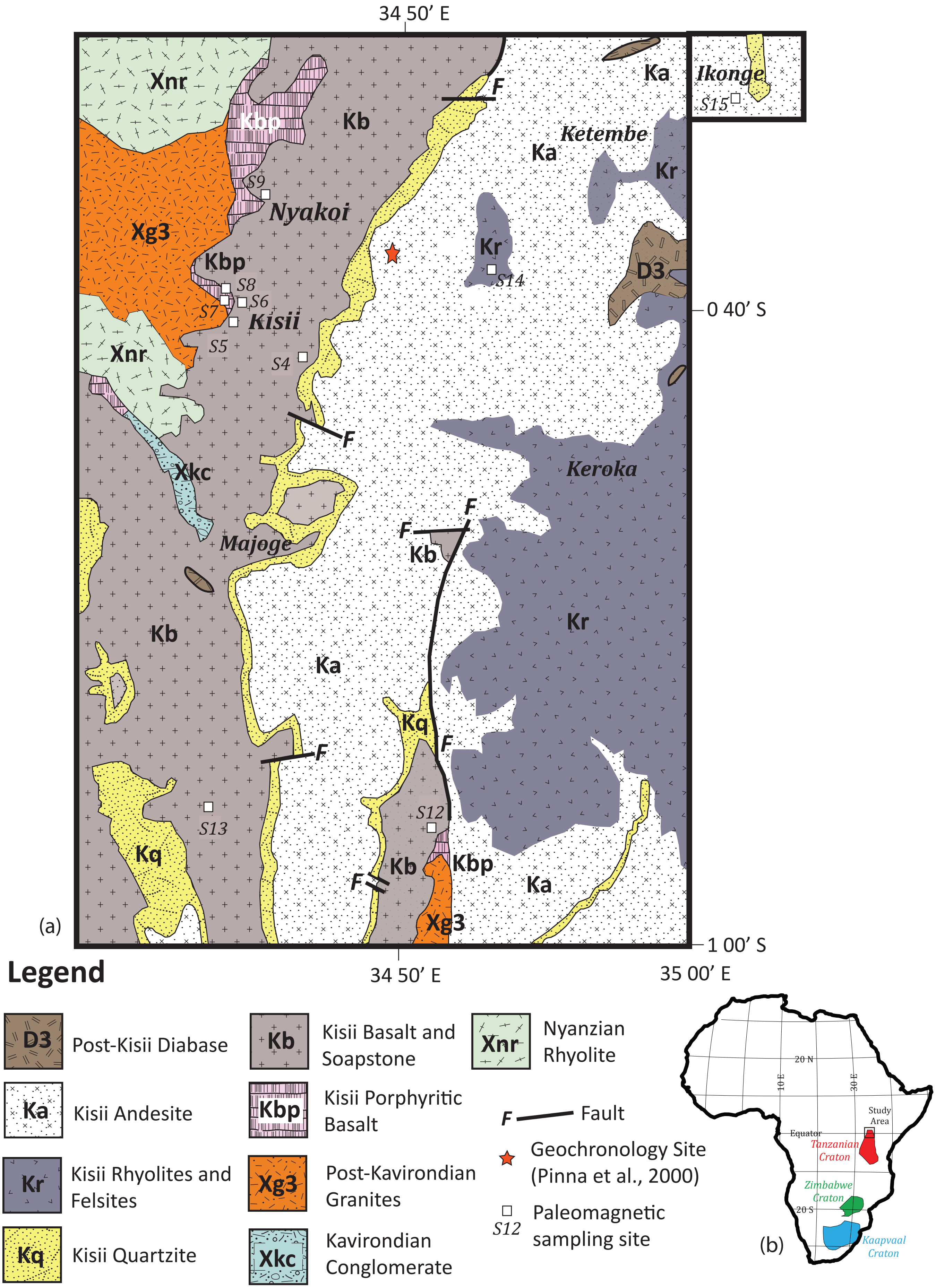

34 50' E
Xnr
Kbp
Kb
F
Ka
Ikonge
S15
Ketembe
Kr
S9
Nyakoi
Xg3
Kbp
S8
S6
S7
Kisii
D3
0 40' S
S14
S5
S4
F
Xkc
Keroka
Majoge
F
F
Kb
Kr
Kb
Ka
Kq
F
F
S12
S13
Kq
Kb
Kbp
Ka
F
Xg3
(a)
1 00' S
34 50' E
35 00' E
Legend
D3
Post-Kisii Diabase
Kb
Kisii Basalt and Soapstone
Xnr
Nyanzian Rhyolite
Ka
Kisii Andesite
Kbp
Kisii Porphyritic Basalt
F
Fault
Kr
Kisii Rhyolites and Felsites
Xg3
Post-Kavirondian Granites
Geochronology Site (Pinna et al., 2000)
Kq
Kisii Quartzite
Xkc
Kavirondian Conglomerate
S12
Paleomagnetic sampling site
20 N
10 E
30 E
Study Area
Equator
Tanzanian Craton
Zimbabwe Craton
20 S
Kaapvaal Craton
(b)

Figure2

Generalized Stratigraphic Relationships in the Kisii Region

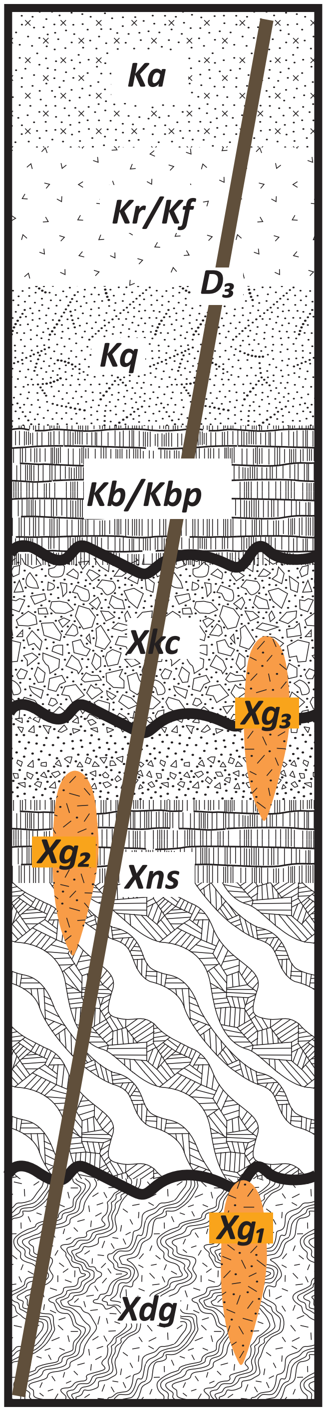

D_3: Post-Kisii dykes <2530 Ma

Ka: Kisii andesite

Kr/Kf: Kisii felsite 2531 Ma

Kq: Kisii quartzite

Kb/Kbp: Kisii basalts and porphyritic basalts.

Xg_3: Post-Kavirondian granites. <2650 Ma and >2531 Ma

Xkc: Kavirondian conglomerate and sedimentary rocks. <2650 Ma

Xg_2: Post-Nyanzian granites ~2650-2680 Ma. Deformation at ~2650 Ma

Xns: Nyanzian System volcanics (rhyolites, basalts, andesites) and banded iron formation. ~2800-2700 Ma

Xg_1: Older granites <3100 Ma and >2800 Ma

Xdg: Dodoman gneisses and local basement schists. >3600 Ma to 3100 Ma

Figure3

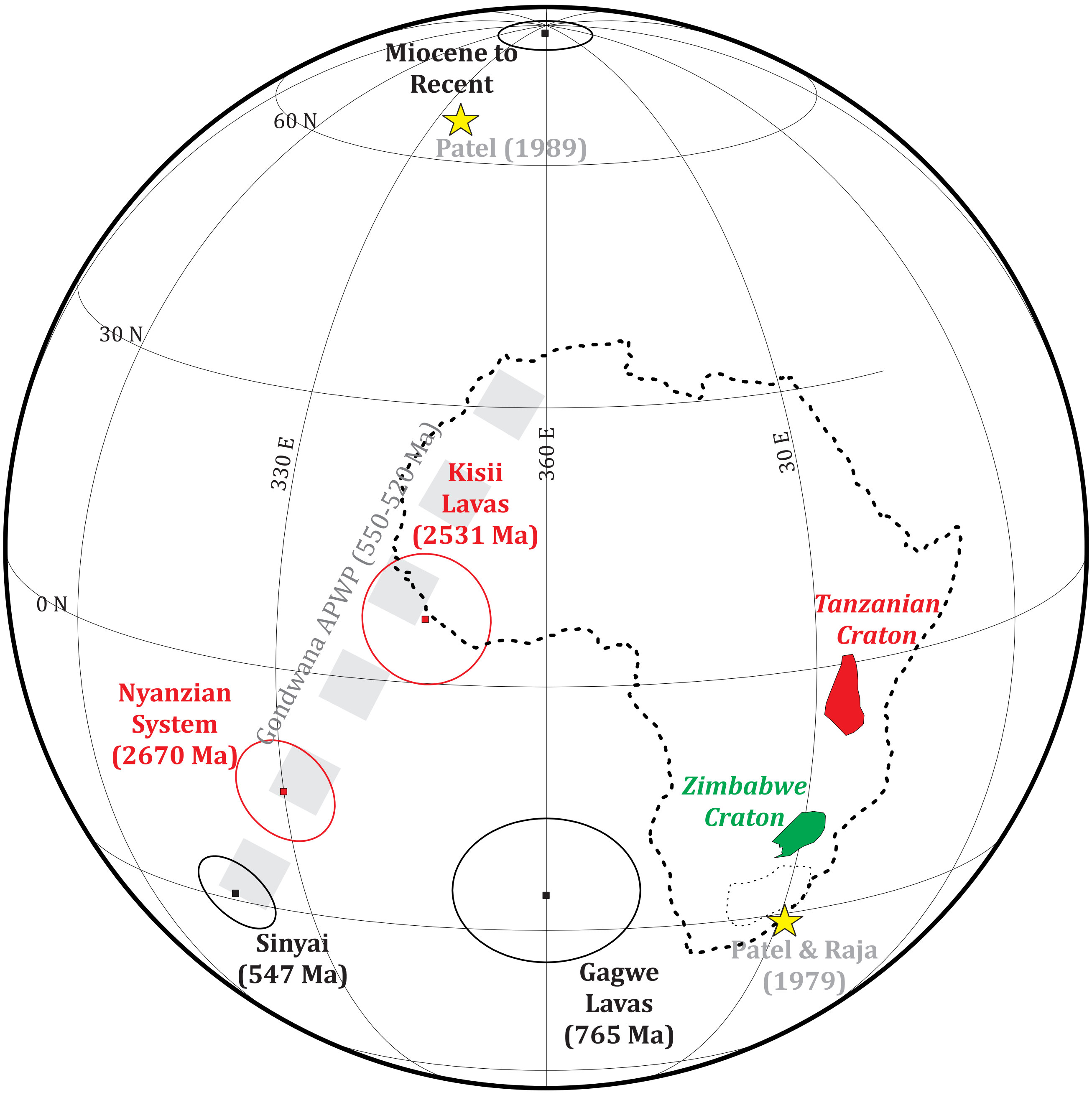

Miocene to Recent
60 N
Patel (1989)
30 N
330 E
360 E
30 E
Gondwana APWP (550-520 Ma)
Kisii Lavas (2531 Ma)
0 N
Tanzanian Craton
Nyanzian System (2670 Ma)
Zimbabwe Craton
Sinyai (547 Ma)
Gagwe Lavas (765 Ma)
Patel & Raja (1979)

Figure4

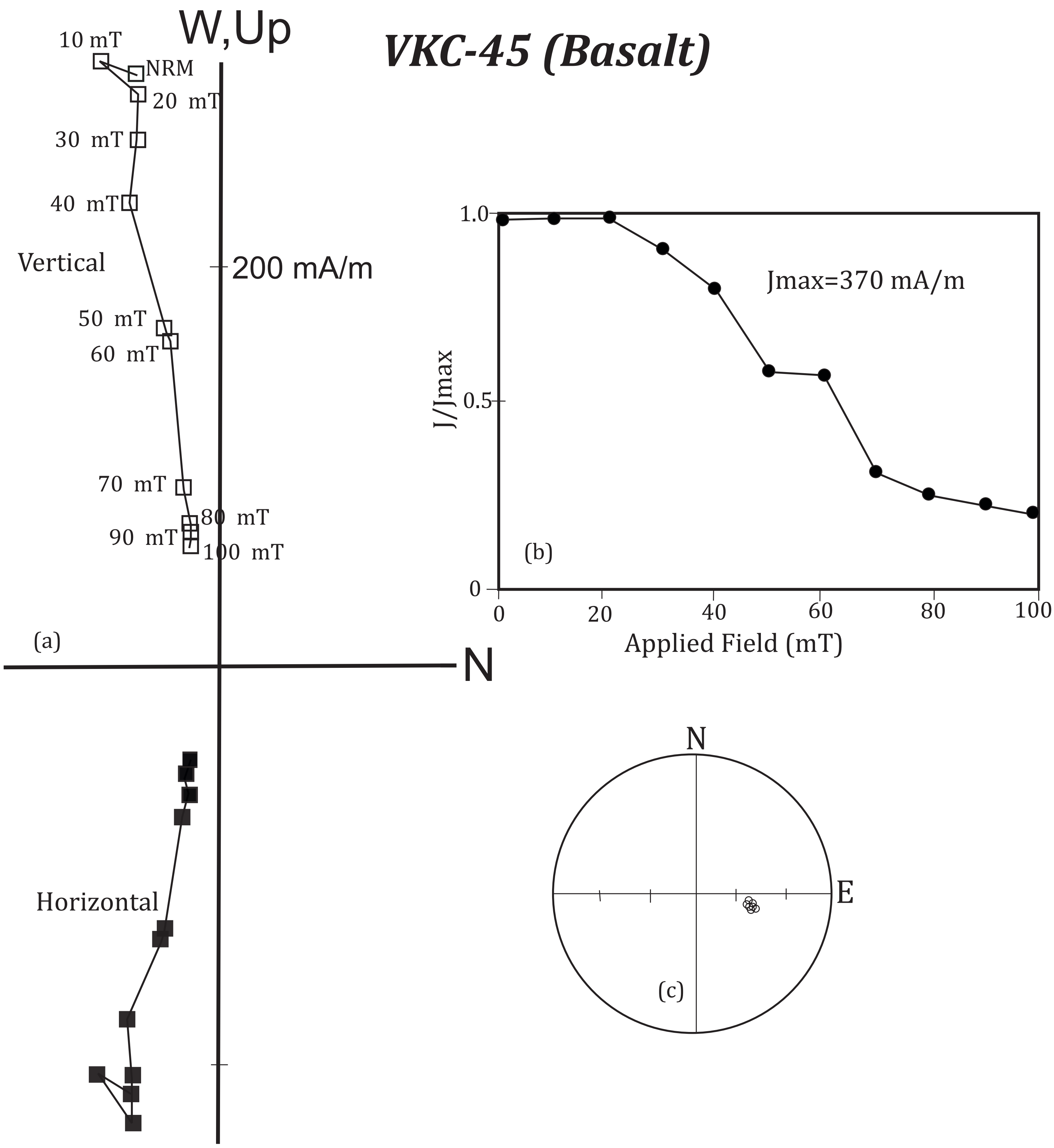

VKC-45 (Basalt)
W,Up
10 mT
NRM
20 mT
30 mT
40 mT
Vertical
200 mA/m
50 mT
60 mT
70 mT
80 mT
90 mT
100 mT
(a)
N
Horizontal
1.0
0.5
0
J/Jmax
Jmax=370 mA/m
(b)
0
20
40
60
80
100
Applied Field (mT)
N
E
(c)

Figure5

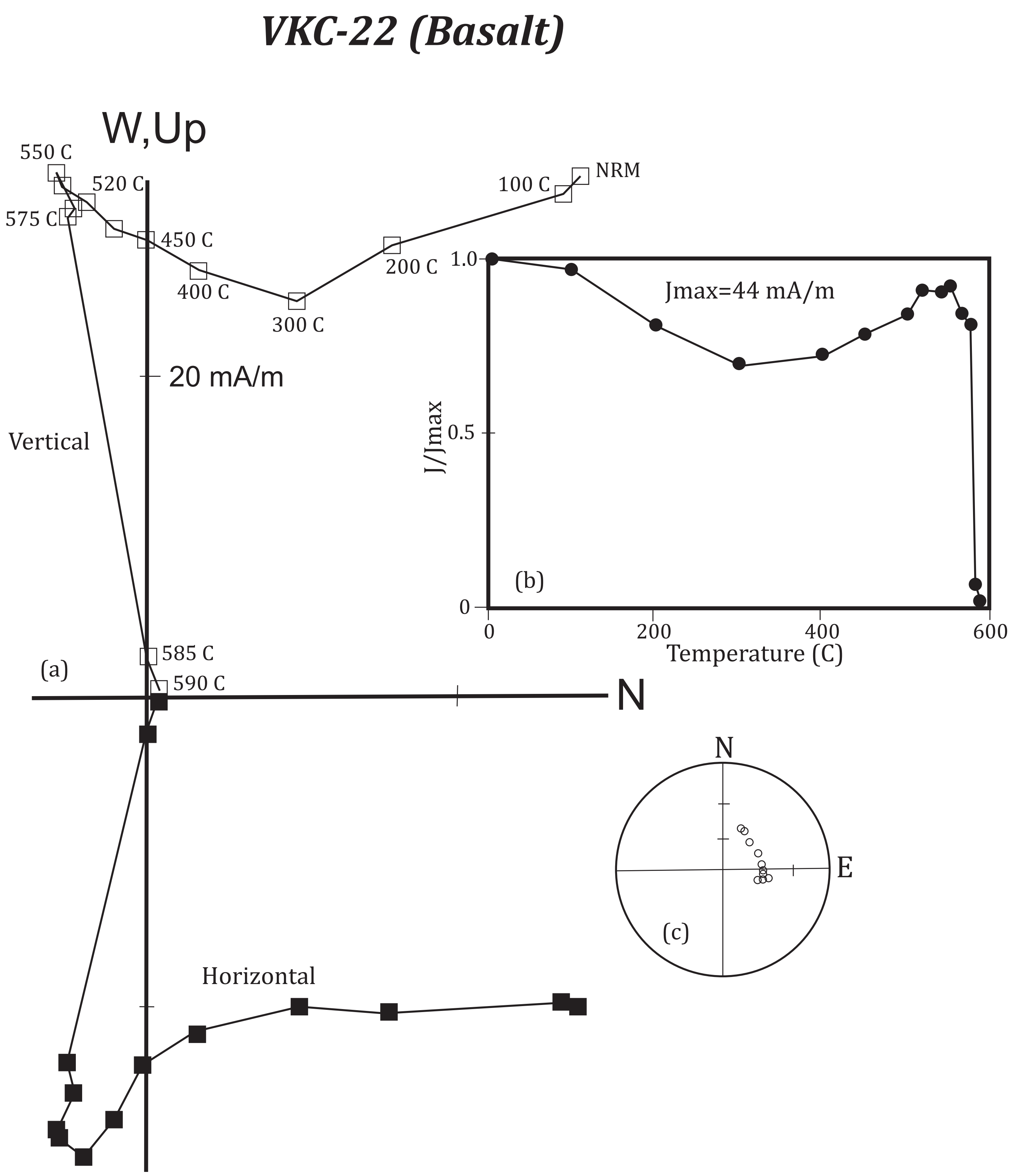
VKC-22 (Basalt)
W,Up
550 C
520 C
575 C
450 C
400 C
300 C
200 C
100 C
NRM
20 mA/m
Vertical
585 C
590 C
(a)
N
Horizontal
1.0
0.5
0
J/Jmax
Jmax=44 mA/m
(b)
0
200
400
600
Temperature (C)
N
E
(c)

Figure6

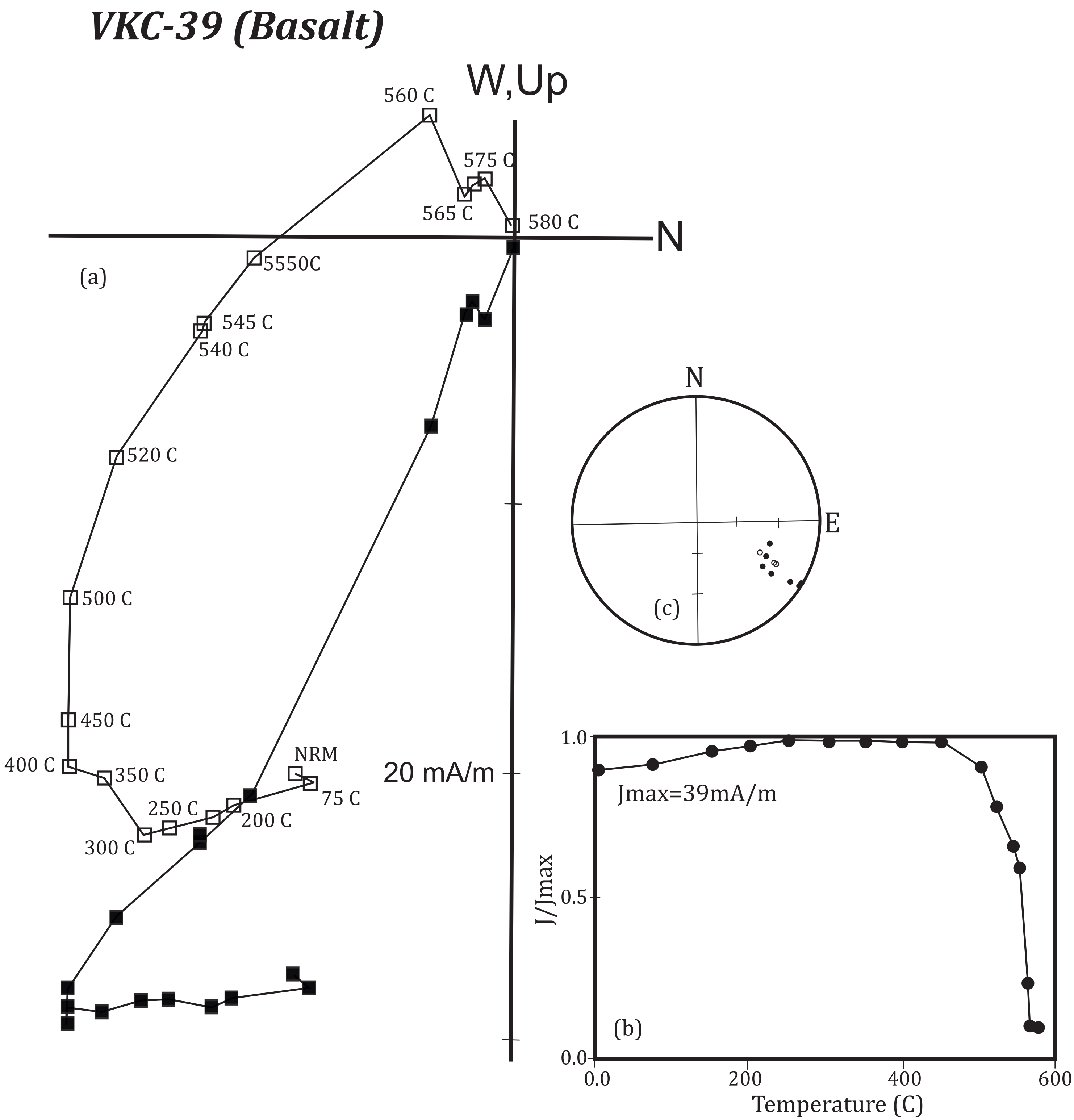
VKC-39 (Basalt)
W,Up
N
560 C
575 C
565 C
580 C
5550C
(a)
545 C
540 C
520 C
500 C
450 C
400 C
350 C
NRM
75 C
250 C
200 C
300 C
20 mA/m
N
E
(c)
1.0
0.5
0.0
J/Jmax
Jmax=39mA/m
(b)
0.0
200
400
600
Temperature (C)

Figure7

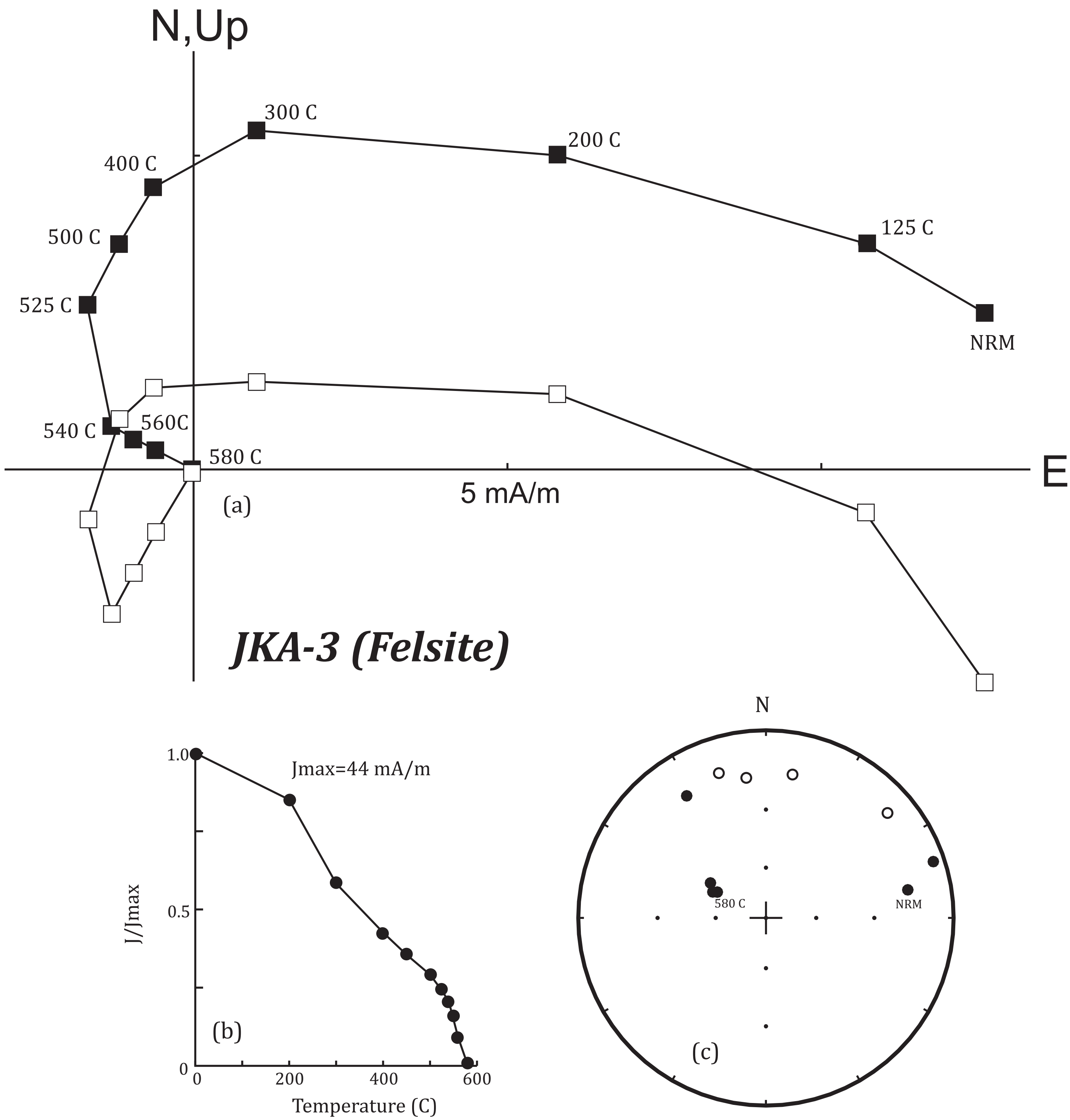

N,Up
300 C
200 C
400 C
500 C
125 C
525 C
NRM
540 C
560C
580 C
E
5 mA/m
(a)
JKA-3 (Felsite)
1.0
Jmax=44 mA/m
J/Jmax
0.5
(b)
0
0
200
400
600
Temperature (C)
N
580 C
NRM
(c)

Figure8

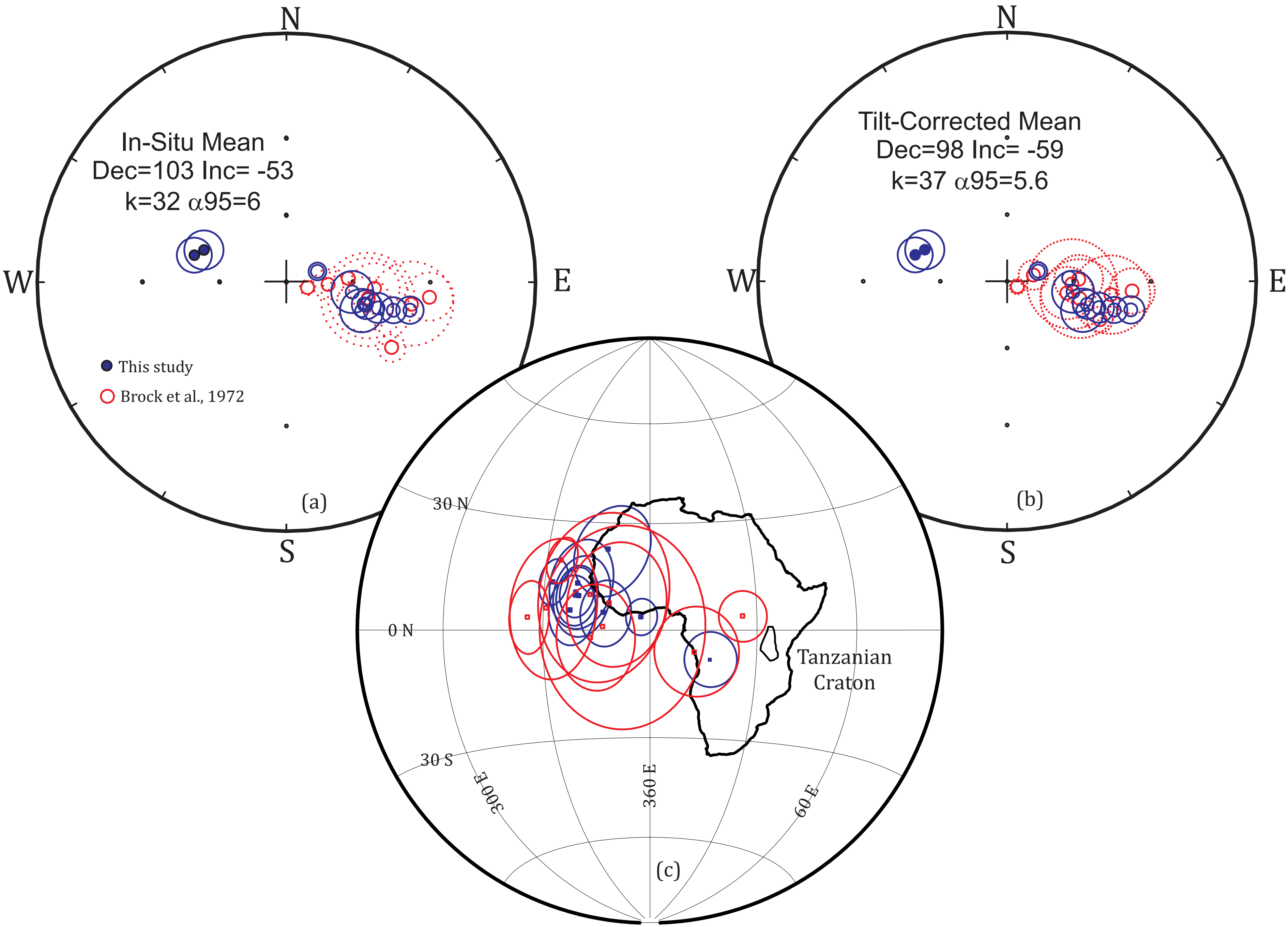

N
W
E
S
In-Situ Mean
Dec=103 Inc= -53
k=32 α95=6
This study
Brock et al., 1972
(a)
N
W
E
S
Tilt-Corrected Mean
Dec=98 Inc= -59
k=37 α95=5.6
(b)
30 N
0 N
30 S
300 E
360 E
60 E
Tanzanian
Craton
(c)

Figure9

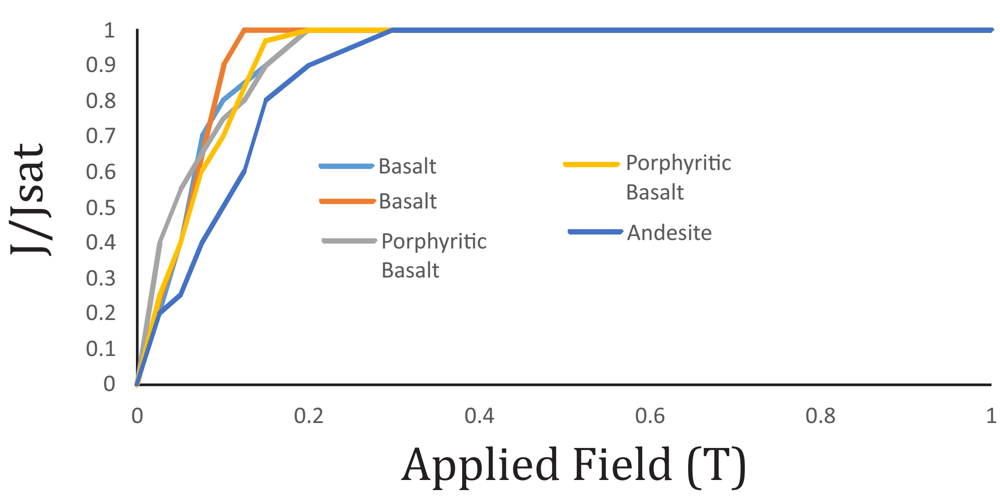
J/Jsat
1
0.9
0.8
0.7
0.6
0.5
0.4
0.3
0.2
0.1
0
0
0.2
0.4
0.6
0.8
1
Applied Field (T)
Basalt
Basalt
Porphyritic Basalt
Porphyritic Basalt
Andesite

Figure10

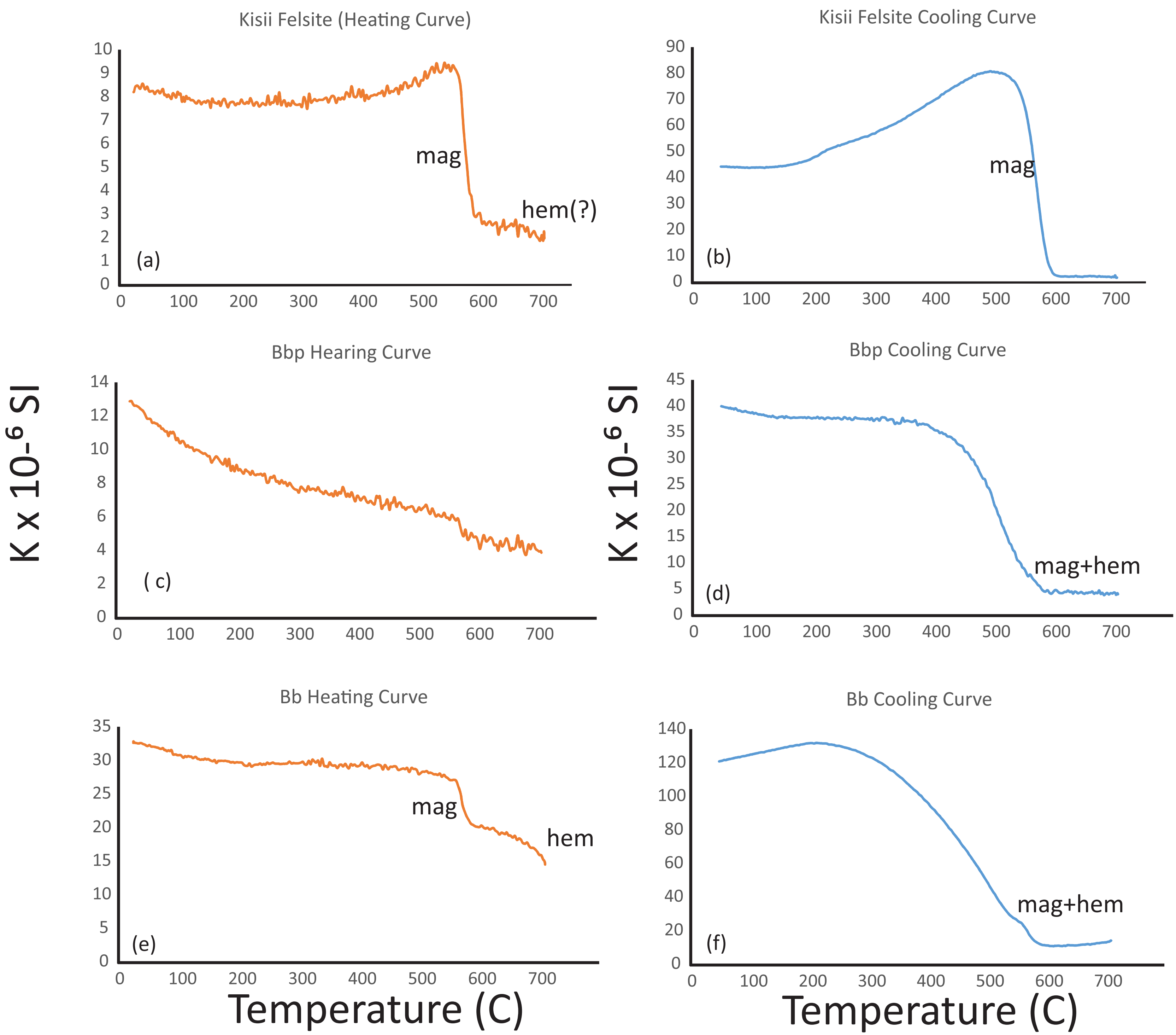
Kisii Felsite (Heating Curve)
mag
hem(?)
(a)
Kisii Felsite Cooling Curve
mag
(b)
Bbp Hearing Curve
(c)
Bbp Cooling Curve
mag+hem
(d)
Bb Heating Curve
mag
hem
(e)
Bb Cooling Curve
mag+hem
(f)
K x 10-6 SI
K x 10-6 SI
Temperature (C)
Temperature (C)

Figure11

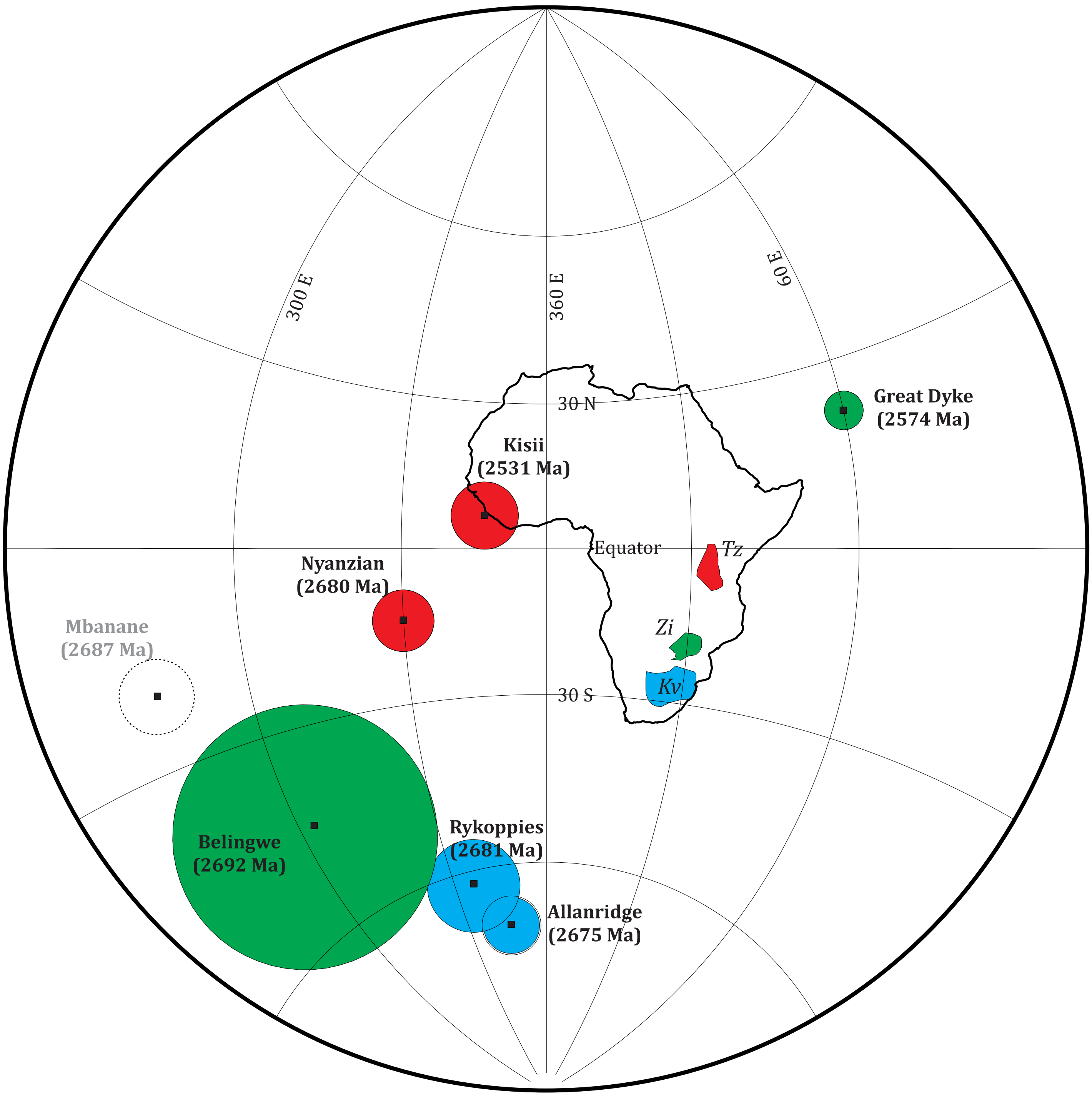
300 E
360 E
60 E
30 N
Equator
30 S
Great Dyke
(2574 Ma)
Kisii
(2531 Ma)
Nyanzian
(2680 Ma)
Mbanane
(2687 Ma)
Belingwe
(2692 Ma)
Rykoppies
(2681 Ma)
Allanridge
(2675 Ma)
Tz
Zi
Kv

Figure12